Experiments on evanescent-wave amplification and transmission using metamaterial structures

Tie Jun Cui,* Xian Qi Lin, Qiang Cheng, Hui Feng Ma, and Xin Mi Yang
Center for Computational Electromagnetics and the State Key Laboratory of Millimeter Waves, Department of Radio Engineering, Southeast University, Nanjing 210096, People's Republic of China
(Received 28 April 2006; revised manuscript received 8 June 2006; published 28 June 2006)

We present a theoretical and experimental study on the evanescent-wave amplification (EWA) and evanescent-wave transmission (EWT) using a waveguide structure. The evanescent waves (or cutoff waves) can be easily generated in a planar substrate integrated waveguide (SIW), which behaves quite similarly to a conventional rectangular waveguide. We insert a structured left-handed material (LHM) that is composed of distributed series capacitors and shunt inductors into a SIW to verify the EWA and EWT phenomena. From both simulation and experimental results on transmission coefficients, we observe that evanescent waves are amplified and transmitted through the structured LHM metamaterial within the frequency band that exhibits negative refraction. We also show that evanescent waves cannot be transmitted if we insert a right-handed microstrip line or distributed capacitor circuit inside the SIW. Such experiments directly confirm the EWA and EWT phenomena in the LHM metamaterial. We notice that there is a discrepancy in internal electric field distributions between theoretical predictions in the ideally homogeneous LHM and experimental observations in the structured metamaterial. We give an explanation for this discrepancy.

DOI: 10.1103/PhysRevB.73.245119 PACS number(s): 78.20.Ci, 41.20.Jb, 42.25.Bs, 84.40.Az

I. INTRODUCTION

Optical or electromagnetic imaging has been studied for centuries and now is still one a very of the most attractive topics. From classical optics theory, there is a limitation on optical imaging: all-optical lenses cannot focus light onto a region smaller than a square wavelength.[1] This limitation is due to the fact that only propagating Fourier spectra emitted from the source can be reconstructed by a conventional lens. The evanescent waves, however, decrease exponentially from the source and tend to zero at the focus point. Hence the conventional lens cannot recover the information of evanescent waves, which results in the one-wavelength resolution in optical imaging.

Recently, a new proposal to construct a "perfect" lens has been investigated theoretically using a metamaterial slab with negative index of refraction.[1] Although such a metamaterial, which was first termed a left-handed material (LHM),[2] does not exist in nature, it has been realized artificially using split-ring resonators and copper strips or inductor-capacitor (*LC*) circuits in microwave frequencies and terahertz optics.[3–7] In the perfect lens, the lossless metamaterial slab which has a negative permittivity $-\epsilon_0$ and a negative permeability $-\mu_0$ can amplify all evanescent waves emitted from the source and recover them at the focus point.[1] Hence the imaging resolution is not limited by the wavelength any more but by the loss of metamaterial. When a small loss exists in the metamaterial slab, a subwavelength imaging can be achieved to form a superlens.[8–11] Because of this surprising property, the perfect lens or superlens has attracted a lot of investigators.

The key point in constructing the perfect lens or superlens is the amplification of evanescent waves by the metamaterial. However, this phenomenon is difficult to verify by experiments. There are two main reasons: (1) it is difficult to generate and measure the evanescent waves; (2) it is difficult to realize a metamaterial slab with small enough loss. One can solve the first difficulty easily using a hollow waveguide, which possesses a cutoff frequency f_c. When the operating frequency is below f_c, the wave "propagates" in the waveguide in an evanescent mode. Recently an experimental study of evanescent-wave enhancement has been reported, performed by inserting a structured metamaterial composed of split-ring resonators[3] (SRRs) inside the rectangular waveguide.[12] In the experiment, only a single-negative-μ metamaterial (SRR) was used, where the evanesent-wave amplification (EWA) phenomenon can only occur at an optimal μ at a specific frequency. Due to the relatively large loss in the SRR metamaterial, the transmission coefficient through the waveguide was not given.[12]

It has been shown that a structured metamaterial composed of *LC* circuits has much smaller loss and has been applied in some new microwave components and antennas.[4,5] However, the *LC*-structured metamaterial is manufactured in the conventional printed circuit board (PCB), which is difficult to combine with the bulk rectangular waveguide. Hence we have to use some kind of planar waveguide, which is also manufactured as a PCB. Recently, a so-called substrate integrated waveguide (SIW) has been developed, using a grounded PCB and via holes, which has a similar behavior as the traditional rectangular waveguide.[13,14] Thus we propose an experimental verification in this paper to verify the EWA and evanescent-wave transmission (EWT) phenomena using an *LC*-structured metamaterial inserted into a SIW.

II. THEORETICAL PREDICTION

First we study the theoretical prediction of evanescent-wave amplification and transmission inside a rectangular hollow waveguide by an ideally homogeneous metamaterial slab, as shown in Fig. 1. The waveguide is infinitely long in the z direction, and has a size of $a \times b$ in cross section, where $b < a$. In the following derivations, the time dependence of $\exp(j\omega t)$ is assumed and suppressed. If the waveguide is

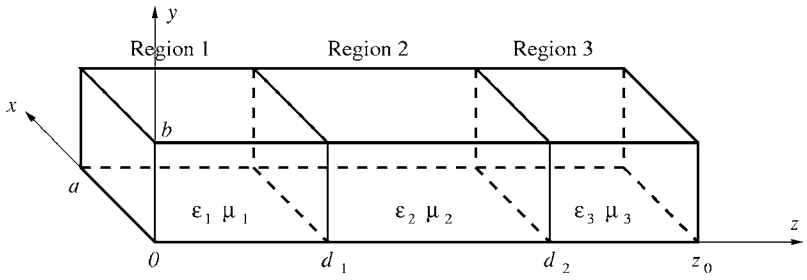

FIG. 1. A rectangular waveguide filled with three-layered media.

filled with a homogeneous medium with the relative permittivity ϵ_{r1} and permeability μ_{r1}, only the dominant TE_{10} mode exists when the working frequency is below the cutoff frequency of the TE_{20} mode. Then the electric field inside the waveguide is easily written as

$$E_y = \frac{-j\omega\mu_0\mu_{r1}}{k_c^2}\frac{\pi}{a}H_{10}\sin\frac{\pi x}{a}e^{-j\beta_1 z}, \tag{1}$$

in which $k_c=\pi/a$ is the cutoff wave number, $\beta_1^2=k_0^2\mu_{r1}\epsilon_{r1}-k_c^2$, and k_0 is the wave number in free space. The cutoff wave number determines a cutoff frequency $f_c=c_0/2a\sqrt{\mu_{r1}\epsilon_{r1}}$, where c_0 is the light speed in free space.

When the waveguide is filled with a dielectric slab with the relative permittivity ϵ_{r2} and permeability μ_{r2} at interfaces $z=d_1$ and $z=d_2$, the electric fields in the regions $z<d_1$, $d_1\le z<d_2$, and $z\ge d_2$ are expressed as

$$E_{1y} = \frac{-j\omega\mu_1}{k_c}H_{10}\sin k_c x(e^{-j\beta_1 z}+Re^{j\beta_1 z}), \tag{2}$$

$$E_{2y} = \frac{-j\omega\mu_2}{k_c}H_{10}\sin k_c x(C^+e^{-j\beta_2 z}+C^-e^{j\beta_2 z}), \tag{3}$$

$$E_{3y} = \frac{-j\omega\mu_3}{k_c}H_{10}\sin k_c xTe^{-j\beta_3 z}, \tag{4}$$

in which R and T are the reflection and transmission coefficients of the slab, and $\beta_2^2=k_0^2\mu_{r2}\epsilon_{r2}-k_c^2$. Using the boundary conditions, we easily obtain

$$R = \frac{R_{12}+R_{23}e^{-j2\beta_2 h}}{1+R_{12}R_{23}e^{-j2\beta_2 h}}e^{-j2\beta_1 d_1}, \tag{5}$$

$$T = \frac{4e^{-j(\beta_2-\beta_1)h}}{(1+P_{12})(1+P_{23})(1+R_{12}R_{23}e^{-j2\beta_2 h})}, \tag{6}$$

$$C^+ = \frac{\mu_1}{\mu_2}\frac{2e^{j(\beta_2-\beta_1)d_1}}{(1+P_{12})(1+R_{12}R_{23}e^{-j2\beta_2 h})}, \tag{7}$$

$$C^- = \frac{\mu_1}{\mu_2}\frac{2R_{23}e^{j(\beta_2-\beta_1)d_1}e^{-j2\beta_2 d_2}}{(1+P_{12})(1+R_{12}R_{23}e^{-j2\beta_2 h})},$$

in which $h=d_2-d_1$ represents the thickness of the dielectric slab, $R_{12}=-R_{23}=(1-P_{12})/(1+P_{12})$ are the Fresnel reflection coefficients at the two boundaries, and $P_{12}=1/P_{23}=\mu_1\beta_2/\mu_2\beta_1$. Here, it has been assumed that regions 1 and 3 have the same permittivity and permeability.

In the special case that $\epsilon_2=\epsilon_1$ and $\mu_2=\mu_1$, we easily obtain $R=0, T=1, C^+=1$, and $C^-=0$. Then the waves inside the waveguide propagate in the form of $\exp(-j\beta_1 z)$. When the frequency is above the cutoff frequency and the medium is lossless, the corresponding propagating wave is totally transmitted without any attenuation; when below the cutoff frequency, the corresponding evanescent wave will decay exponentially.

Now we consider the reflection and transmission when the middle dielectric slab is a metamaterial. In the case of a perfect lens $\epsilon_2=-\epsilon_1$ and $\mu_2=-\mu_1$, we study the propagating and evanescent waves separately. For propagating waves ($f>f_c$), we have $\beta_2=-\beta_1, P_{12}=1, P_{23}=1$, and $R_{12}=R_{23}=0$, and furthermore we obtain $R=0$ and $T=e^{j2\beta_1 h}$, which means that propagating waves can be transmitted totally without any attenuation. For evanescent waves ($f<f_c$), however, we have $\beta_2=\beta_1=-j\alpha_1, P_{12}=-1, P_{23}=-1$, and furthermore $R=0$ and $T=e^{2\alpha_1 h}$. Hence, the evanescent waves can be amplified by the perfect lens. At the exterior image point $z=2h$, we clearly see that all propagating and evanescent information at $z=0$ can be recovered, which is quite similar to Pendry's prediction[1] in the perfect lens in free space.

If the metamaterial is lossy and the real parts of ϵ_{r2} and μ_{r2} are retarded to those of $-\epsilon_{r1}$ and $-\mu_{r1}$, the amplification of evanescent waves is still expected. Figure 2(a) illustrates the transmission coefficients when ($\epsilon_{r2}=-5-j0.1$, $\mu_{r2}=-1.5-j0.1$) and ($\epsilon_{r2}=-6-j0.2$, $\mu_{r2}=-1.8-j0.2$), in which $a=23.84$ mm, $\epsilon_{r1}=4.1$, $\mu_{r1}=1$, $d_1=2.63$ mm, $d_2=17.01$ mm, and the observation point is fixed at $z=19.64$ mm. Clearly, a significant amplification of evanescent waves is observed in both cases. As a comparison, the transmission coefficient without the LHM slab is also given. Below the cutoff frequency ($f_c=3.1$ GHz), the evanescent waves cannot propagate. Above the cutoff frequency, nearly total transmission occurs.

In order to show the EWA phenomenon further, Figs. 2(a) and 2(c) give the electric field distributions along the z axis when $x=a/2$ at the frequency of 2 GHz. From Fig. 2(b), we observe an exponential enhancement of the evanescent wave at the first interface and then an exponential decay inside the LHM slab followed by another growth at the second interface, and finally an exponential decay outside the LHM region. As a comparison, the field distribution without the LHM slab is also given, which shows an exponential decay along the observation line, as expected. From Fig. 2(c), we notice increased phase distributions throughout the LHM region, which indicates wave propagation at negative phase velocities. Throughout the RHM regions, the phases are

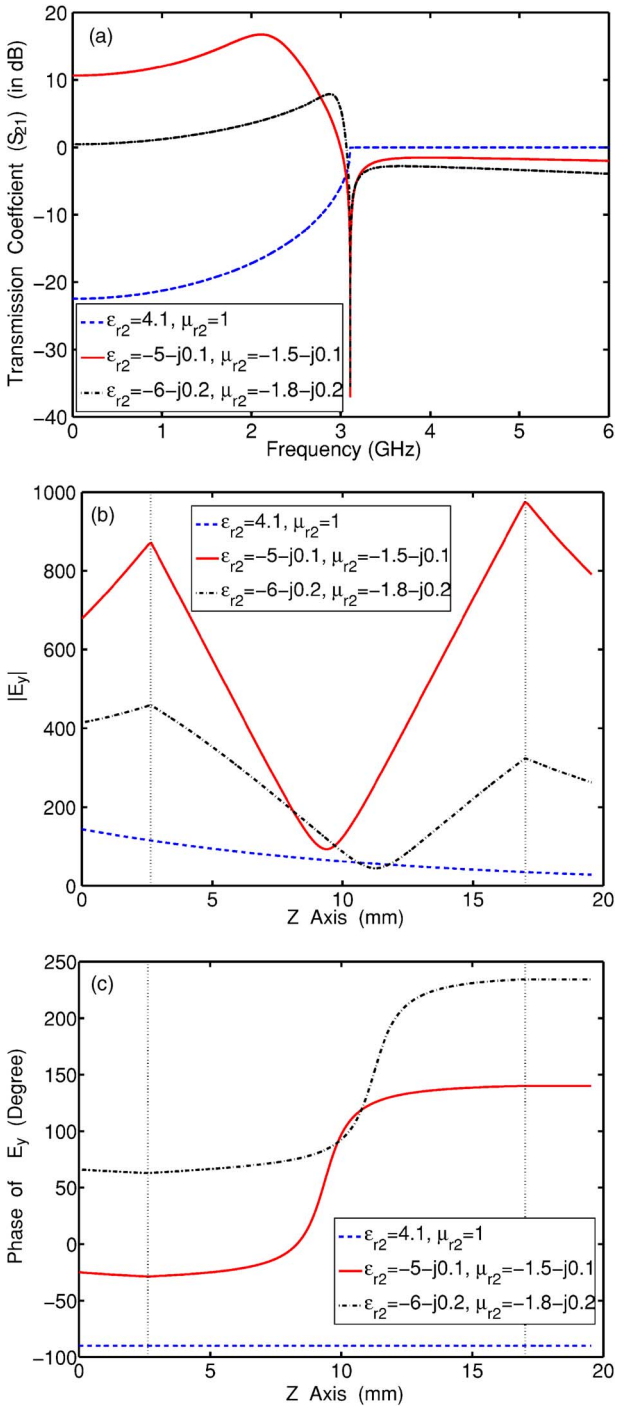

FIG. 2. (Color online) Theoretical prediction results for the rectangular waveguide filled with a homogeneously lossy LHM slab, where a=23.84 mm, d_1=2.63 mm, d_2=17.01 mm, z=19.64 mm (ϵ_{r1}=4.1, μ_{r1}=1), (ϵ_{r2}=−5−j0.1, μ_{r2}=−1.5−j0.1), or (ϵ_{r2}=−6−j0.2, μ_{r2}=−1.8−j0.2). The cutoff frequency is f_c=3.1 GHz. (a) Transmission coefficients. (b) Amplitudes of internal electric fields. (c) Phases of internal electric fields.

nearly constant due to the evanescent nature of the waves.

III. EXPERIMENTS AND SIMULATIONS

In order to verify the above phenomenon, we design an experiment system using a SIW and *LC*-structured metamaterial, as shown in Fig. 3(a). It has been shown that a SIW exhibits quite similar behaviors as the traditional rectangular waveguide.[13,14] Here we use a smooth transition to connect the SIW section with standard microstrip lines (50 Ω). The microstrip lines are then connected to an Agilent E8363B Network Analyzer through subminiature version A (SMA) connectors to measure the reflection and transmission properties.

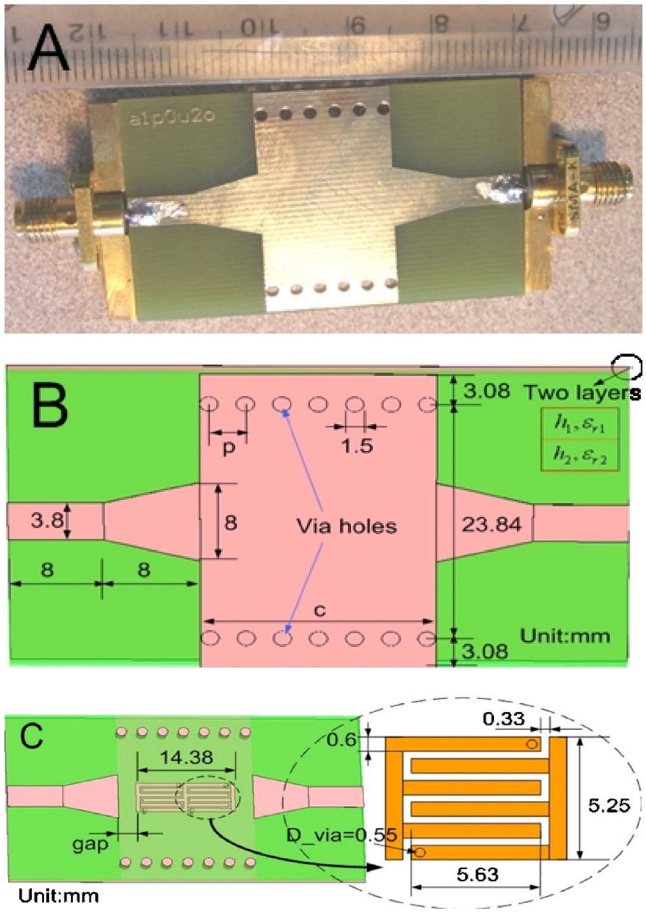

FIG. 3. (Color online) (a) Photograph of the experiment system, where an *LC*-structured metamaterial or a standard microstrip line is inserted inside the SIW. (b) Detailed structure of SIW. (c) Detailed structure of the CRLH metamaterial, which is inserted at the interface of the two PCB layers inside the SIW.

Unlike the conventional single-layered SIW,[13,14] the SIW in our experiments is particularly fabricated using a two-layered PCB, which is made of the common FR4 material. The two layers have the same dielectric constant 4.1 and tangent loss 0.025. The first layer is 0.5 mm thick and the second layer is 1.55 mm thick, as shown in Fig. 3(b). We insert the structured metamaterial or other structures at the interface of the two PCB layers.

The SIW region is covered by copper sheets on the top and bottom surfaces. We use periodic via holes to form the sidewalls of the SIW for easy fabrication in the PCB. The diameter of each via is 1.5 mm, and the period of via holes is p=3.016 mm. The SIW section has a width of a =23.84 mm and different lengths c depending on the inner structures. We have shown that such a SIW behaves quite

similarly to the conventional rectangular waveguide with the same width[13,14] since the period p is small enough. Hence the cutoff frequency of the dominant TE_{10} mode inside the SIW is 3.1074 GHz. To make a good matching between the SIW and the standard microstrip lines, two 8-mm-long tapered transitions have been used, as shown in Fig. 3(b).

The detailed structure of the metamaterial is illustrated in Fig. 3(c), which is inserted at the interface of the two PCB layers inside SIW. The metamaterial consists of two unit cells with a total length of 14.38 mm. We set a gap between the metamaterial and the transition so that evanescent waves must "propagate" along the gap before entering the metamaterial. In our experiments, the gap is chosen as 2.63 and 1 mm, respectively. The unit cell of the metamaterial is composed of an interdigital capacitor and two via holes, as shown in Fig. 3(c). The latter are equivalent to two shunt inductors. Such a formation is in fact a variation of the composite right and left-handed (CRLH) structure[5,15] with a more compact size. We have designed the unit cell carefully so that the resonant frequency for a negative index of refraction is below the SIW cutoff frequency and the metamaterial possesses a small loss. Under the chosen parameters shown in Fig. 3(c), we have shown that the frequency band to reach negative refraction is around 1.74 GHz.

We designed six experimental boards for measurements and simulations. In the first one, the SIW is empty and nothing is inserted ($c=19.64$ mm). In the second one, a right-handed microstrip line is inserted in the SIW, which is printed on the interface of the two PCB layers, as shown in Fig. 4(a). Here, $c=19.64$ mm, and the gap between the microstrip line and the transition is 2.63 mm. In the third and fourth boards, the two-cell metamaterial is inserted in the SIW with gap of 2.63 and 1 mm, respectively. In the fifth one, two-cell interdigital capacitors are inserted inside the SIW with a gap of 2.63 mm, as illustrated in Fig. 4(b). We remark that the interdigital capacitor is exactly the same as that in Fig. 3(c). However, the two via holes representing the shunt inductors do not exist. In the sixth board, a four-cell metamaterial is inserted in the SIW with a gap of 2.63 mm [see Fig. 4(c)].

We will measure the scattering S parameters S_{21} of the above structures to study the transmission properties. All measurements are performed using the Agilent E8363B network analyzer, where the starting frequency is 100 MHz. We choose the ending frequency as 6 GHz so that only the dominant TE_{10} exists in the SIW.

For the empty SIW, the measurement transmission coefficient is illustrated in Fig. 5 (solid line). As expected, no evanescent waves below the cutoff frequency ($f_c=3.1074$ GHz) can propagate through the waveguide due to their exponential decay. The smaller the frequency is, the larger the decay. Such a phenomenon is exactly the same as we predicted in the theoretical analysis shown in Fig. 2(a). Above the cutoff frequency, we observe that all propagating waves have nearly total transmission, in which the small attenuation is caused by the dielectric loss in the PCB. As a comparison, we also simulated the S parameter S_{21} using the CST MICROWAVE STUDIO, as shown in Fig. 5 (dash-dotted line). A good agreement has been observed between the measured and simulated results.

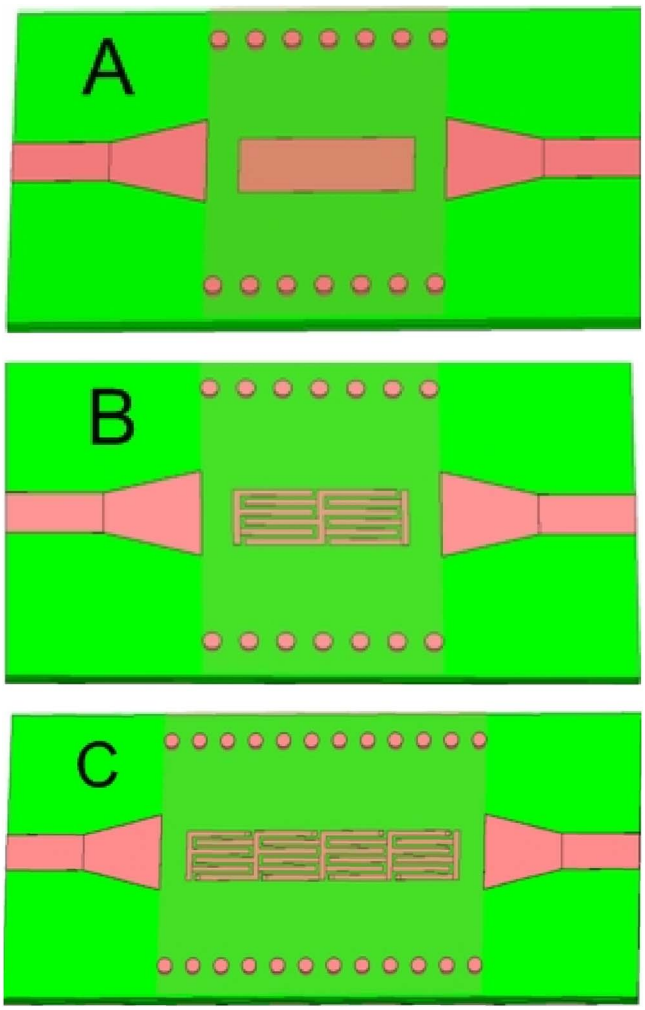

FIG. 4. (Color online) (a) A right-handed microstrip line is inserted inside the SIW. (b) Two-unit interdigital capacitors are inserted inside the SIW, where the interdigital capacitor is exactly the same as that in Fig. 3(c). Note that the two via holes do not exist. (c) Four-unit CRLH structure is inserted inside the SIW.

When we insert the microstrip line (a right-handed transmission line) inside the SIW, the measured and simulated transmission coefficients are shown in Fig. 5 (dashed and dotted lines). It is obvious that the transmission coefficients with and without the microstrip line are nearly the same. Hence the evanescent behavior of the SIW below the cutoff frequency is maintained when there is an additional right-handed transmission line inside the SIW.

When we insert the two-cell-structured metamaterial with the gap of 2.63 mm (a CRLH transmission line) inside the SIW, we clearly observe a good transmission of evanescent waves around the frequency of 1.74 GHz, as shown in Fig. 6. Such a frequency band just corresponds to the negative refraction of the metamaterial. In the measurement and simulation results, the resonant frequencies are located at 1.734 and 1.743 GHz, and the corresponding transmission coefficients reach −3.51 and −3.85 dB, respectively, which are in excellent agreement. Obviously, the transmission coefficient of the evanescent wave at the resonant frequency has been enlarged significantly by the metamaterial from −23 dB (in an empty or right-handed SIW) to −3.51 dB.

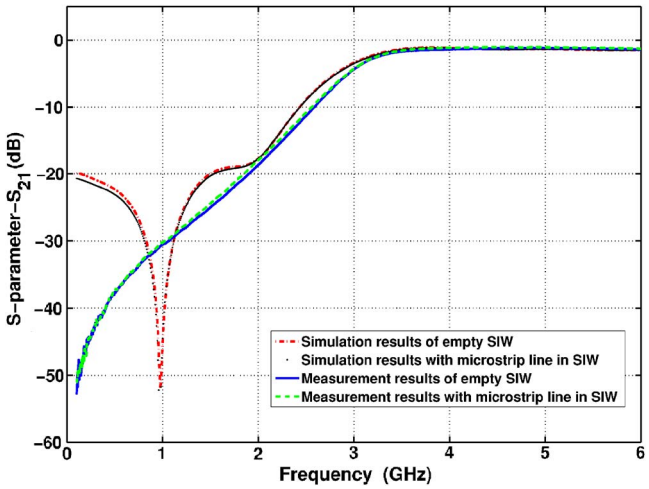

FIG. 5. (Color online) Simulated and measured transmission coefficients in the frequency range from 100 MHz to 6 GHz when the SIW is empty or has a right-handed microstrip line inserted. Below the cutoff frequency (f_c=3.1 GHz), the evanescent waves cannot propagate. Above the cutoff frequency, good transmission occurs, in which the small attenuation is caused by the dielectric loss of the PCB.

The gaps in all experiment setups are very important in the verification of EWA and EWT phenomena. Without the gaps, the evanescent waves cannot be excited because the input signal can always propagate along the microstrip lines or LHM structure. With the gaps, the designed experiment verifies the interaction of evanescent waves instead of signals to the LHM circuits.

If we reduce the gap between the LHM metamaterial and transition to 1 mm, the measured and simulated transmission coefficients are demonstrated in Fig. 7. We again observe the amplification and transmission of evanescent waves in the same frequency band. In this case, the measured S_{21} has been increased to −2.56 dB since the evanescent wave has a smaller decay along the shorter gap, as we expected.

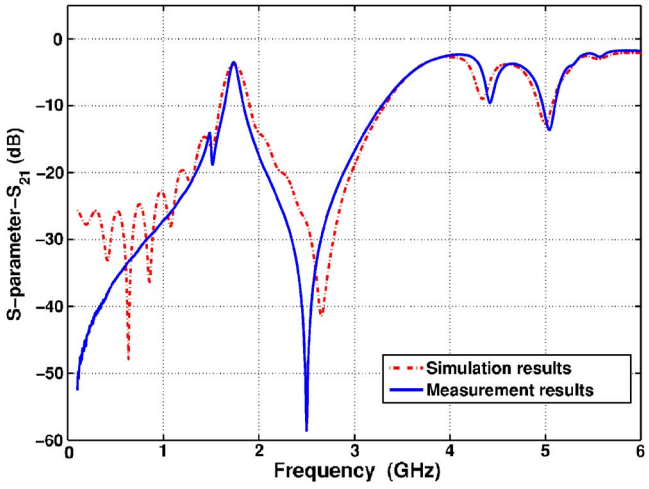

FIG. 6. (Color online) Simulated and measured transmission coefficients in the frequency range from 100 MHz to 6 GHz when a two-unit CRLH structure is inserted inside the SIW, where the gap to the transition is 2.63 mm. We clearly observe an amplification of evanescent waves around the frequency of 1.74 GHz, which corresponds to the negative refraction of the metamaterial.

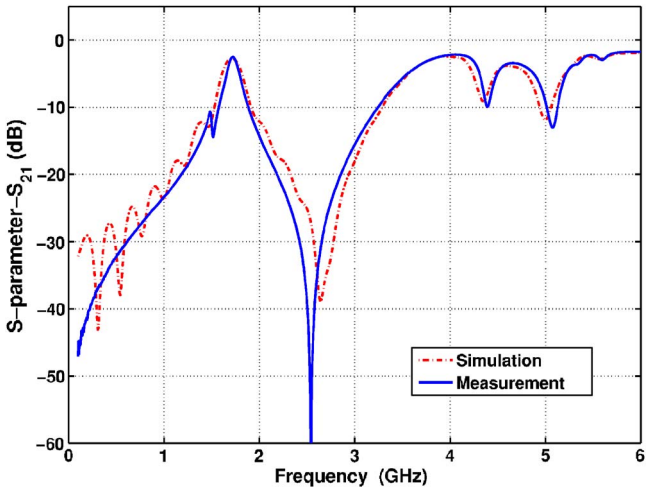

FIG. 7. (Color online) Simulated and measured transmission coefficients in the frequency range from 100 MHz to 6 GHz when a two-unit CRLH structure is inserted inside the SIW, where the gap to the transition is 1 mm. A similar phenomenon to that in Fig. 6 is observed.

It is very important to inspect if the big "jump" in the transmission coefficient within the cutoff frequency range shown in Figs. 6 and 7 is due to the amplification of evanescent waves, which is closely related to the negative refraction, or to a simple filter-resonant behavior which has no relation to the negative refraction. To do so, we study the wave propagation and field distribution inside the SIW at the frequency of 1.74 GHz. Figures 8(a) and 8(b) illustrate the distributions of electric fields along an observation line from the left end to the right end of the structure shown in Fig. 3(c) (solid lines). The observation line is parallel to the via-hole array, passing the microstrip line at the left end ($z \in [-16,-8]$ mm), the left transition section ($z \in [-8,0]$ mm), the left gap ($z \in [0,2.63]$ mm), the metamaterial region ($z \in [2.63,17.01]$ mm), and the right gap, transition, and microstrip line ($z \in [17.01,35.64]$ mm). In the vertical direction, the observation line is located in the middle between the LHM structure and lower waveguide surface; in the horizontal direction, the observation line is located in the center of the LHM structure to capture the left-handed properties.

From Fig. 8(a), we observe that the electric field is decayed along the right-handed regions (the microstrip lines, transitions, and gaps). At the interface to enter the LHM structure (z=2.63 mm), there is a peak similar to a surface wave, as shown in the solid line in Fig. 8(a). Inside the LHM structure, the field values become very large due to the electromagnetic resonance needed to generate the negative refraction. At the other interface z=17.01 mm, a small peak is also observed. From Fig. 8(b), we observe decreased phase distributions along the right-handed transmission lines (microstrip lines and transitions along $z \in [-16,0]$ mm and $z \in [19.64,35.64]$ mm), which indicates the wave propagation at positive phase velocities. Throughout the gaps inside the

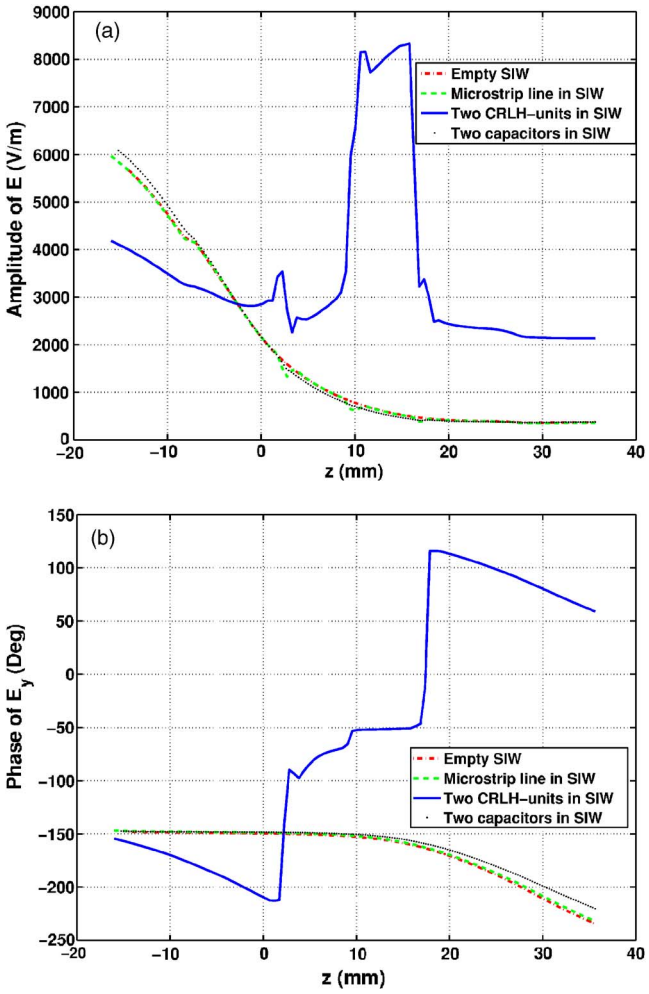

FIG. 8. (Color online) Distributions of electric fields along an observation line from the left end to the right end shown in Fig. 3(b) when a two-unit CRLH structure is inserted inside the SIW. (a) Amplitude. (b) Phase.

waveguide ($z \in [0, 2.63]$ mm and $z \in [17.01, 19.64]$ mm), the phases are nearly constant. Throughout the LHM region inside the SIW ($z \in [2.63, 17.01]$ mm), however, we clearly observe an increased phase distribution, which implies a negative phase velocity in this region. This phenomenon is coincident with the theoretical prediction given in Fig. 2(c). Hence we can verify that the *LC*-structured metamaterial shows negative refraction, and the big jump in the transmission coefficient in Figs. 6 and 7 is due to the amplification of evanescent waves, as illustrated in Fig. 8(a).

As a comparison, we have also plotted the field distributions inside the empty SIW and the SIW with the microstrip line in Figs. 8(a) and 8(b) (dash-dotted and dashed lines). Clearly, the field distributions inside the SIW decay exponentially, which is the same as the theoretical prediction in Fig. 2(a), and the inserted right-handed microstrip line does not affect the evanescent behavior of the SIW.

The above phenomena can be further verified if we insert a complicated structure, two series interdigital capacitors, inside the SIW. As shown in Fig. 4(b), the structure is nearly the same as that in Fig. 3(c) except for the lack of via holes.

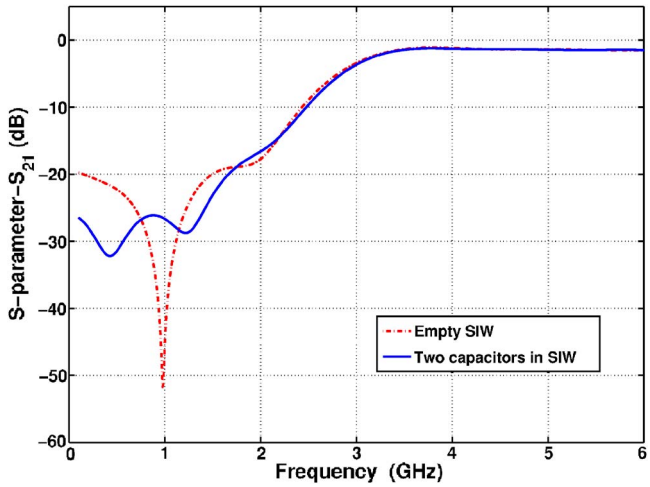

FIG. 9. (Color online) Comparison of transmission coefficients when the SIW is empty and has two-unit interdigital capacitors inserted. A similar phenomenon to that in Fig. 5 is observed.

Figures 8(a), 8(b), and 9 illustrate the corresponding internal field distributions (dotted lines) and transmission coefficient (solid line), which are very close to those of the empty SIW. Hence the inserted interdigital capacitors do not affect the evanescent behavior either. In other words, only the LHM structure which exhibits negative refraction can amplify the evanescent waves.

In order to demonstrate the above conclusions further, we make another experiment using a four-cell LHM metamaterial inserted in the SIW, as shown in Fig. 4(c), which has a length of 28.76 mm and a gap of 2.63 mm to the transition. The measured and simulated transmission coefficients are illustrated in Fig. 10, from which the EWT phenomenon is again observed in the frequency band from 1.65 to 2 GHz (larger than −20 dB). We have examined this frequency band, which corresponds to the negative refraction of the LHM structure. From Fig. 10, we also notice that the ampli-

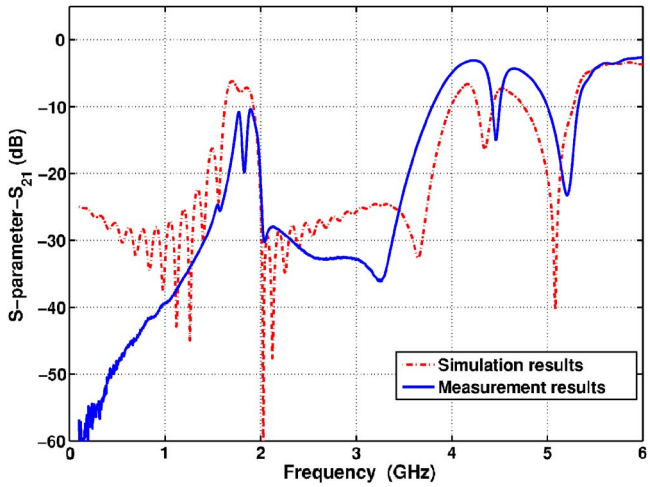

FIG. 10. (Color online) Simulated and measured transmission coefficients in the frequency range from 100 MHz to 6 GHz when a four-unit CRLH structure is inserted inside the SIW. A similar phenomenon is observed to that in the two-cell case.

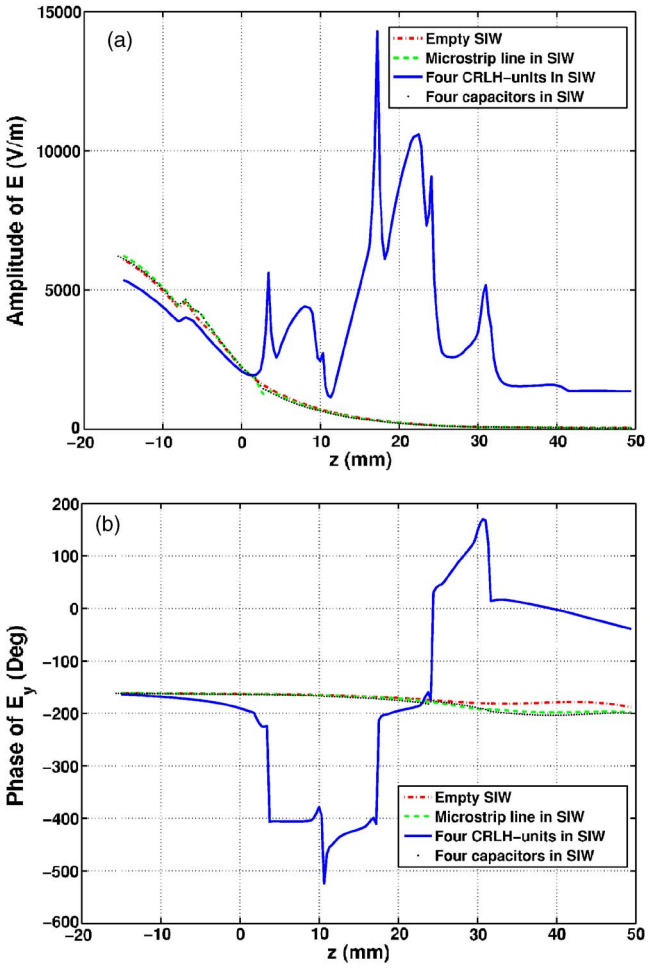

FIG. 11. (Color online) Distributions of electric fields along an observation line from the left end to the right end shown in Fig. 3(b) when a four-unit CRLH structure is inserted inside the SIW. (a) Amplitude. (b) Phase.

fication level of the transmission coefficient has been decreased by approximately 7 dB in the measurement data compared to that in Fig. 6. This is because the evanescent wave travels a longer way (28.76 mm) in the lossy LHM metamaterial.

As in the case of two cells, we finally investigate the wave propagation and field distribution inside a four-cell-structured SIW at the frequency of 1.81 GHz. Figures 11(a) and 11(b) illustrate the field distributions along a similar observation line to the previous one. From Fig. 11(a), the electric field is decayed when $z<2.63$ mm in the evanescent mode. Near the interfaces of the LHM structure, $z=2.63$ and 30.79 mm, there are two peaks of surface waves. Inside the LHM structure, there are four evident resonances due to the four unit cells. From Fig. 11(b), we observe an increased phase distribution throughout the LHM region, which indicates a negative phase velocity. Thus we further verify the negative refraction of the LHM structure and the corresponding amplification and transmission of evanescent waves.

For easy comparison, the field distributions inside the empty SIW, the SIW with longer microstrip line, and the SIW with four series interdigital capacitors are also given in Figs. 11(a) and 11(b). Clearly, the field distributions in all three cases decay exponentially and the inserted right-handed microstrip line and interdigital capacitors do not affect the evanescent behavior of the SIW. Only the LHM structure which exhibits negative refraction allows evanescent-wave transmission.

From Figs. 2, 8, and 11, we clearly see that the phase distributions of internal electric fields inside a SIW with structured metamaterials are similar to those inside a rectangular waveguide filled with an ideally homogeneous LHM. However, the amplitude distributions shown in Figs. 8(a) and 11(a) behave quite differently from the theoretical prediction and SRR experiments.[12] As we know, a homogeneous LHM has been assumed in the theoretical prediction, which does not exist in nature. In real cases, all artificial LHMs are made of periodic structures like SRRs and printed *LC* circuits, where strong locally resonant fields exist.

In the SRR experiment,[12] we notice that the local fields were detected "far" away from the SRR structures, where the observation holes are 21 mm away from the horizontal SRRs, and at least 7 mm away from the vertical SRRs. Hence, the resonances appearing in SRRs have small influ-

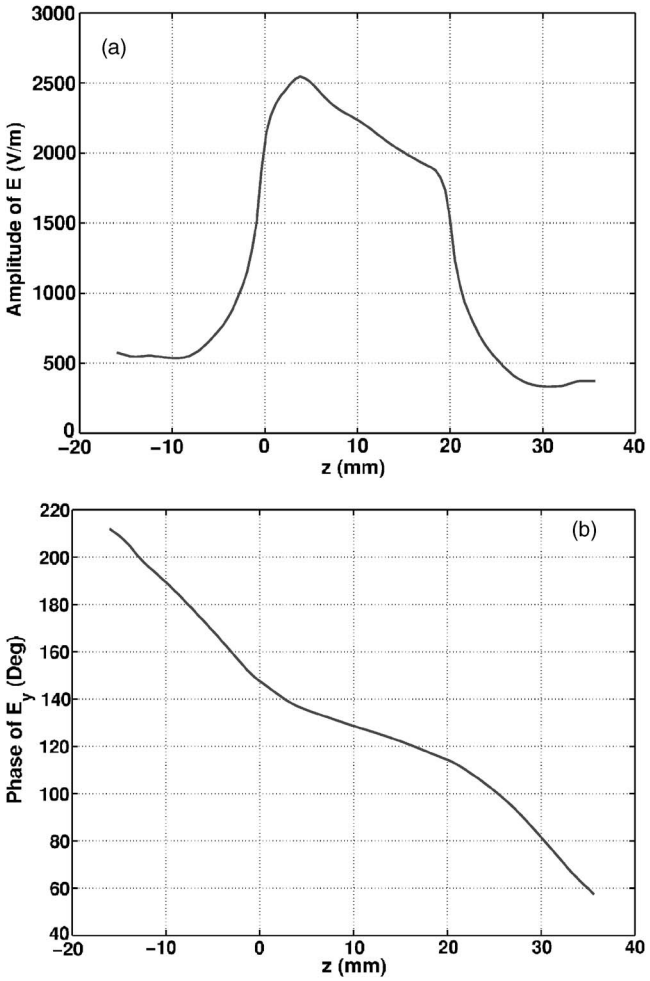

FIG. 12. Distributions of electric fields along an observation line "far" from the CRLH structure at a distance of 5.96 mm, where two-unit CRLH cells are inserted inside the SIW. (a) Amplitude. (b) Phase.

ence on the observation fields. Even so, we still observe small jumps of the fields at some observation holes close to the vertical SRRs, as shown in Fig. 4 in Ref. 12.

In our experiments, however, the observation line is only 0.775 mm away from the LHM structures. Because of this very close distance, the strong local resonance in capacitors and inductors affects the observation fields significantly, as shown in Figs. 8(a) and 11(a). To verify that the physical reason for these big peaks in these figures is the strong local resonance, we simulated the field distributions along a new observation line which is "far" from the LHM structure (5.96 mm in the horizontal direction), as illustrated in Fig. 12. Clearly, the peaks in the amplitude distribution shown in Fig. 8(a) disappear because the effect of local resonance becomes weaker. However, the fields far away from the LHM structure do not have left-handed properties [see Fig. 12(b)], and only the fields inside and near the LHM structure are left handed.

IV. CONCLUSIONS

In conclusion, our experimental results confirm the amplification and transmission of evanescent waves at microwave frequencies through an *LC*-structured metamaterial. It is important to notice that the designed experiment verifies the interaction of evanescent waves instead of signals in the LHM circuits due to the small gap.

ACKNOWLEDGMENTS

This work was supported in part by the National Basic Research Program (973) of China under Grant No. 2004CB719802, in part by the National Science Foundation of China for Distinguished Young Scholars under Grant No. 60225001, in part by the National Science Foundation of China under Grant No. 60496317, and in part by the National Doctoral Foundation of China under Grant No. 20040286010.

*Email address: tjcui@seu.edu.cn

[1] J. B. Pendry, Phys. Rev. Lett. **85**, 3966 (2000).
[2] V. G. Veselago, Sov. Phys. Usp. **10**, 509 (1968).
[3] R. A. Shelby, D. R. Smith, and S. Schultz, Science **292**, 77 (2001).
[4] A. Grbic, G. V. Eleftheriades, Phys. Rev. Lett. **92**, 117403 (2004).
[5] C. Caloz and T. Itoh, *Electromagnetic Metamaterials: Transmission Line Theory and Microwave Applications* (Wiley, New York, 2004).
[6] C. Sirtori, Nature (London) **417**, 132 (2002).
[7] S. Linden, C. Enkrich, M. Wegener, J. Zhou, T. Koschny, and C. M. Soukoulis, Science **306**, 1351 (2004).
[8] X. S. Rao and C. K. Ong, Phys. Rev. B **68**, 113103 (2003).
[9] S. A. Cummer, Appl. Phys. Lett. **82**, 1503 (2003).
[10] R. Merlin, Appl. Phys. Lett. **84**, 1290 (2004).
[11] T. J. Cui, Z. C. Hao, X. X. Yin, W. Hong, and J. A. Kong, Phys. Lett. A **323**, 484 (2004).
[12] B. I. Popa and S. A. Cummer, Phys. Rev. E **73**, 016617 (2006).
[13] D. Deslandes and K. Wu, IEEE Microw. Wirel. Compon. Lett. **11**, 68 (2001).
[14] F. Xu, Y. Zhang, W. Hong, K. Wu, and T. J. Cui, IEEE Trans. Microwave Theory Tech. **51**, 2221 (2003).
[15] Z. X. Zhang and S. J. Xu, Microwave Opt. Technol. Lett. **45**, 422 (2005).